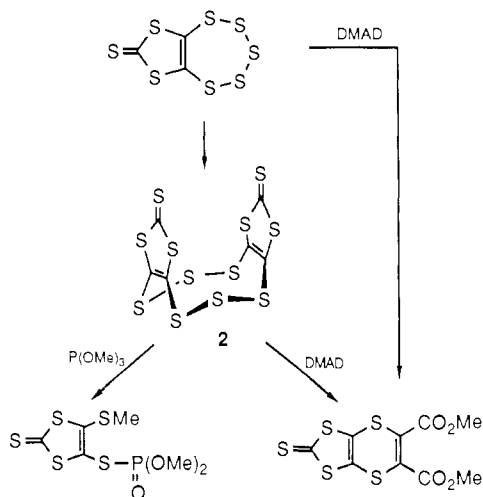
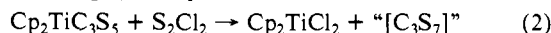


Scheme I



410 mg of yellow solids obtained in this way were examined by EI-MS and IR which indicated the absence of hydrocarbons (eq 2). The CH_2Cl_2 soluble portion of the reaction mixture was



filtered through silica gel to remove Cp_2TiCl_2 ; concentration of this filtrate gave 120 mg of yellow crystalline solids identified as C_3S_8 by mass spectrometry, IR, and elemental analysis.¹³

Attempts to grow single crystals of C_3S_8 by slow evaporation of its CS_2 solutions gave well-formed orange prisms which proved to be C_6S_{12} (**2**).¹⁴ This new compound is insoluble in all solvents tested; it can however be obtained in pure form directly from the reaction of $\text{Cp}_2\text{TiC}_3\text{S}_5$ with S_2Cl_2 by washing the resulting precipitate with CS_2 . Solutions of C_3S_8 appear unstable with respect to S_8 and **2**. The EI mass spectrum of **2** does not show peaks for the parent ion, but the fragmentation pattern is distinct from that for C_3S_8 . The IR spectra of C_3S_8 and **2** are also distinct, especially in the $\nu_{\text{S-S}}$ region below 510 cm^{-1} .

The molecular structure of C_6S_{12} is shown in Figure 1.¹⁵ The molecule adopts a crown structure with approximate C_{2v} symmetry. The average S-S bond distances (2.061 Å) and S-S-S angles (106.8°) are very similar to the corresponding values for orthorhombic S_8 .¹⁶ The striking aspects of the structure are nearly eclipsed and mutually parallel (11.85°) C_3S_5 units with an interplanar distance of 3.88 Å for S(6) and S(10). The two C_3S_5 subunits are well suited for van der Waals' interaction since the electronegativities of carbon and sulfur are nearly the same.¹⁷ The delocalized bonding in the C_3S_5 moieties should enhance the polarizability of its constituent atoms which in turn would strengthen this interaction. The structure of **2** and its formation from C_3S_8 indicate that the latter is a simple polysulfide derivative

(13) C_3S_8 : Anal. Calcd for C_3S_8 : C, 12.33; S, 87.67. Anal. Calcd for C_3S_7 : C, 13.83; S, 86.00. Found: C, 12.66; S, 86.16. EIMS 292 (M^+ , 20), 256 (S_8^+ , 7), 228 ($\text{M}^+ - 2\text{S}$, 77); IR $\nu_{\text{C-S}}$ = 1056 (vs), $\nu_{\text{S-S}}$ = 478, 464, 451 (m). The distinction between the S_7 and the S_8 formulations rests on the mass spectrometry; however, there are no established examples of $\text{C}_2(\text{sp}^2)\text{S}_4$ rings, but $\text{C}_2(\text{sp}^2)\text{S}_5$ rings are common. See ref 18.

(14) C_6S_{12} , **2**: Anal. Calcd for C_6S_{12} : C, 15.79; S, 84.21. Found: C, 16.16; S, 84.37. EIMS m/e (intensity) 328 ($\text{M}^+ - 4\text{S}$, 20), 292 (C_3S_8^+ , 20), 256 (S_8^+ , 17), 240 (C_4S_6^+ , 65); IR (KI) $\nu_{\text{C-S}}$ = 1067, 1060 (vs), $\nu_{\text{C-S}}$ = 511, 505 (s), $\nu_{\text{S-S}}$ = 469, 448 cm^{-1} (m).

(15) X-ray crystallography of C_6S_{12} : orange-red crystal, $0.2 \times 0.2 \times 0.4$ mm, orthorhombic, $P2_12_12_1$ (D_2 - No. 19); $a = 9.645$ (2) Å, $b = 7.933$ (2) Å, $c = 19.432$ (4) Å, $V = 1486.8$ (6) Å³; $Z = 4$, $\rho_{\text{calcd}} = 2.040 \text{ g/cm}^3$. Diffraction data: Syntex P2₁ automated four-circle diffractometer. Mo radiation ($K\alpha = 0.71073$ Å), no filters or attenuators, range $3.0 < 2\theta < 54.0^\circ$ for $+h+k+l$ and $3.0 < 2\theta < 15.0^\circ$ for $\pm h \pm k \pm l$, 2296 reflections consisting of 1911 unique data, 1588 of which were defined as observed ($I > \sigma(2.85I)$); corrected for anomalous dispersion, absorption, Lorentz and polarization effects. Least-squares refinement of 1588 independent reflections converged at $R = 0.028$ and $R_w = 0.032$.

(16) Donohue, J. *The Structures of the Elements*; John Wiley and Sons: New York, 1974; p 324.

(17) Williams, A. F. *A Theoretical Approach to Inorganic Chemistry*; Springer Verlag: Berlin, 1979.

of the 1,3,2-dithiacyclopentenethione (Scheme I). Organic compounds with seven-membered 1,2- C_2S_5 rings are known.¹⁸

Preliminary studies have shown that C_6S_{12} is reactive. Treatment of dichloromethane suspensions of **2** with tributylphosphine followed by dimethylacetylenedicarboxylate (DMAD) gives $\text{C}_3\text{S}_5\text{C}_2(\text{COOMe})_2$, isolated as pale yellow crystals.¹⁹ Suspensions of C_6S_{12} in toluene dissolve upon addition of an excess of $\text{P}(\text{OMe})_3$. After evaporation and recrystallization from toluene/ether we obtained the thiophosphonate²⁰ (Scheme I).

In summary we have developed a synthesis of two new carbon sulfides via the titanium-promoted transfer of 1,3,2-dithiacyclopentenethione groups. The new compounds have considerable synthetic potential as precursors to C-S polymers, coordination complexes, and new organosulfur compounds.

Acknowledgment. This research was supported by the National Science Foundation. We thank Jayantha Amarasekera for helpful comments and preliminary experiments.

Supplementary Material Available: Tables of atomic coordinates, thermal parameters, and bond angles and distances (2 pages); tables of observed and calculated structure factors (9 pages). Ordering information is given on any masthead page.

(18) Fëher, F.; Langer, M. *Tetrahedron Lett.* **1971**, 2125. Fëher, F.; Langer, M.; Volkert, R. *Z. Naturforsch.* **1972**, 27B, 1006. Chenard, B. L.; Harlow, R. L.; Johnson, A. L.; Vladuchick, S. A. *J. Am. Chem. Soc.* **1985**, 107, 3871.

(19) Anal. Calcd for $\text{C}_9\text{H}_6\text{O}_4\text{S}_5$: C, 31.95; H, 1.78; S, 47.34. Found: C, 31.56; H, 1.69; S, 47.54. ¹H NMR (CDCl_3) 3.87 ppm; IR (KBr) $\nu_{\text{C-S}}$ = 1063 cm^{-1} ; EIMS (70 eV) m/e 338 (M^+ , 100).

(20) Anal. Calcd for $\text{C}_6\text{H}_6\text{O}_3\text{PS}_5$: C, 22.50; H, 2.81; S, 50.00. Found: C, 22.53; H, 2.81; S, 50.45. ¹H NMR (CDCl_3) 3.91 ppm (d, OCH_3 , $J(\text{P,H}) = 12.9$ Hz), 2.54 (s, SCH_3); ³¹P{¹H} NMR (CH_2Cl_2) 18.86 ppm (vs 85% H_3PO_4); IR (KBr) $\nu_{\text{C-S}}$ = 1063, $\nu_{\text{P=O}}$ = 1261 cm^{-1} ; FD-MS (8 mA) m/e 320 (M^+ , 100).

An ab Initio Investigation of the Double Proton Shift in Azophenine

M. Katharine Holloway*

Molecular Systems Department
Merck Sharp & Dohme Research Laboratories
West Point, Pennsylvania 19486

Charles H. Reynolds*

Computer Applications Research
Rohm and Haas Company
Spring House, Pennsylvania 19477

Kenneth M. Merz, Jr.

Department of Chemistry and
Department of Molecular and Cellular Biology
The Pennsylvania State University
University Park, Pennsylvania 16802

Received October 13, 1988

The automerization of 1,4-diamino-3,6-diimino-1,4-cyclohexadiene, **1a**, is an example of a degenerate double proton shift, as depicted in Figure 1. Based on kinetic and deuterium isotope effects on the rearrangement of the tetraphenyl derivative, azophenine (**1b**), Limbach et al.¹ initially suggested that both hydrogens move simultaneously in a single concerted step, i.e., $\mathbf{1} \rightarrow [\mathbf{4}]^\ddagger \rightarrow \mathbf{1}$. However, subsequent AM1 calculations by Dewar and Merz² disputed this mechanism, suggesting instead that classical automerization occurs through a two-step mechanism, i.e., $\mathbf{1} \rightarrow$

(1) Limbach, H.-H.; Hennig, J.; Gerritzen, D.; Rumpel, H. *J. Chem. Soc., Faraday Discuss.* **1982**, 74, 229.

(2) Dewar, M. J. S.; Merz, K. M., Jr. *J. Mol. Struct. (THEOCHEM)* **1985**, 124, 183.

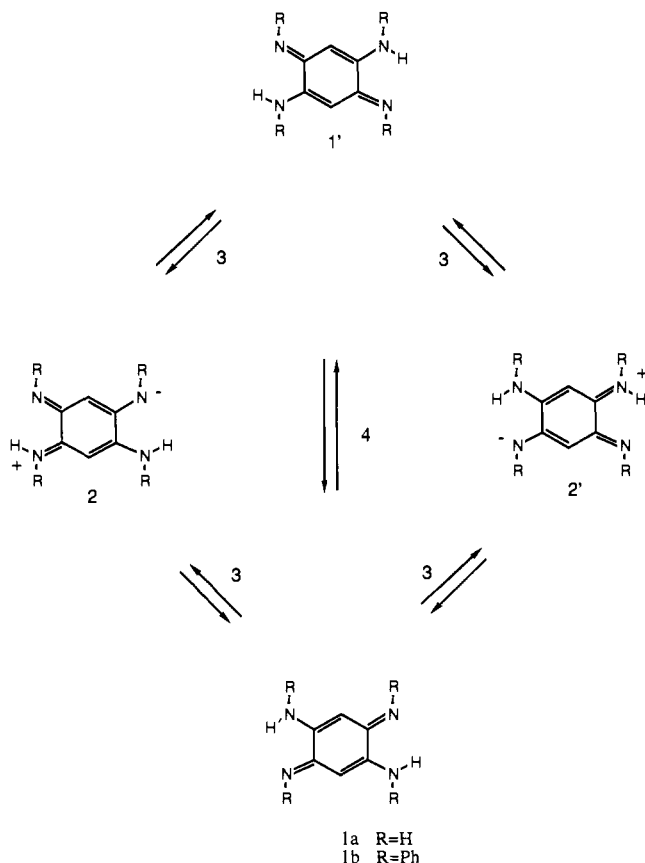


Figure 1. Azophenine automerization pathways.

$[3]^\ddagger \rightarrow 2 \rightarrow [3]^\ddagger \rightarrow 1$. The AM1 calculations strongly favored the two-step over the concerted reaction pathway, and, in addition, the maximum along the concerted pathway (**4a**) was a hilltop (second-order saddle point) not a transition state on the AM1 potential surface. Since double proton shifts of this type are of general interest, we have re-examined the potential surface for automerization of **1a** using ab initio molecular orbital theory.

All species in this study were calculated using the restricted Hartree-Fock (HF) procedure. Semiempirical calculations were carried out using the AM1³ method, as implemented in the AMPAC package.⁴ Ab initio calculations were performed using the 3-21G basis set and the MP2 method, as implemented in the GAUSSIAN86 package.⁵ All 3-21G stationary points were characterized by calculating vibrational frequencies.

The AM1 geometries² for **1a-4a** were recalculated and used as initial geometries for the 3-21G calculations, thus saving considerable time by eliminating the need to do an extensive search of the potential surface at the more expensive 3-21G level. Indeed, the optimized 3-21G geometries are quite similar to the optimized AM1 geometries with average differences in the bond lengths and angles of 0.02 Å and 2.5°, respectively.⁶ This close correspondence has been reported previously by Thiel⁷ and indicates the generality with which AM1 may be used to scan a potential surface for subsequent study by ab initio methods.

(3) Dewar, M. J. S.; Zoebisch, E. G.; Healy, E. F.; Stewart, J. J. P. *J. Am. Chem. Soc.* **1985**, *107*, 3902.

(4) (a) Lynn, L. L.; Pierce, T. H.; Reynolds, C. H. *QCPE Bulletin* **1987**, *7*, 37 (program No. 523, IBM version). (b) Dewar Research Group; Stewart, J. J. P. *QCPE Bulletin* **1986**, *6*, 24a (program No. 506, VAX version modified for an Alliant FX/80).

(5) Frisch, M. J.; Binkley, J. S.; Schlegel, H. B.; Raghavachari, K.; Melius, C. F.; Martin, R. L.; Stewart, J. J. P.; Bobrowicz, F. W.; Rohlfing, C. M.; Kahn, L. R.; Defrees, D. J.; Seeger, R.; Whiteside, R. A.; Fox, D. J.; Fluder, E. M.; Topiol, S.; Pople, J. A. Carnegie-Mellon Quantum Chemistry Publishing Unit, Pittsburgh, PA, 1984 (IBM 3090 and Alliant FX/80 versions).

(6) A table comparing the 3-21G and AM1 optimized geometries is available as Supplementary Material.

(7) (a) Thiel, W. *J. Am. Chem. Soc.* **1981**, *103*, 1413. (b) Schroeder, S.; Thiel, W. *J. Am. Chem. Soc.* **1986**, *108*, 7985.

Table I. 3-21G//3-21G and MP2/3-21G//3-21G Calculated Total Energies (au) for **1a-4a**^a

	3-21G//3-21G	MP2/3-21G//3-21G	AM1
1a	-447.110846007 (0.0)	-448.05037908 (0.0)	0.0
2a	-447.081190648 (18.6)	-448.02564039 (15.5)	22.4
3a	-447.070687929 (25.2)	-448.02281407 (17.3)	50.1
4a	-447.045550387 (41.0)	-448.00837015 (26.4)	88.0

^aRelative energies in kcal/mol are given in parentheses. The AM1³ relative heats of formation in kcal/mol are listed for comparison.

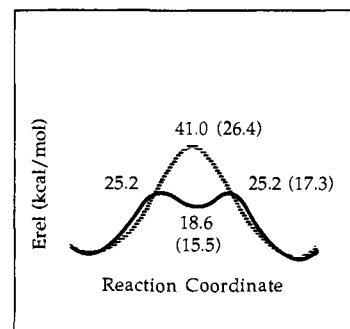


Figure 2. A schematic representation of the 3-21G reaction profiles for the concerted (dashed line) and two-step (solid line) double proton shift in **1a**. MP2/3-21G//3-21G values are given in parentheses.

The 3-21G and MP2/3-21G//3-21G total energies as well as the AM1 relative heats of formation for **1a-4a** are given in Table I; a schematic representation of the concerted and two-step reaction profiles is depicted in Figure 2. The 3-21G calculations agree with AM1 in predicting that the two-step mechanism is more favorable than the concerted mechanism and that the maximum on the concerted pathway **4a** is a hilltop (two imaginary frequencies) not a transition state. One of the imaginary vibrations corresponds to synchronous interconversion between **1a** and **1a'**, while the other corresponds to synchronous interconversion between **2a** and **2a'**. Since a hilltop cannot be involved in the automerization mechanism, the ab initio and AM1 results together provide a strong argument against concerted double proton transfer as a viable classical pathway in azophenine automerization. These results are consistent with recent experimental and theoretical evidence for a two-step mechanism in the automerization reactions of porphyrin⁸⁻¹⁰ and azophenine.^{11,12}

For the two-step mechanism, the 3-21G activation barrier (25 kcal/mol) is much smaller than the AM1 activation barrier (50 kcal/mol). This is not terribly surprising, since AM1 appears³ to share the well-known propensity of MNDO¹³ to overestimate activation barriers involving intramolecular migration of hydrogen. The 3-21G activation barrier is further reduced to 17 kcal/mol with the inclusion of electron correlation at the MP2 level. However, the MP2/3-21G//3-21G barrier is still too large to explain the experimental rate of automerization ($E_{act} \sim 10$ kcal/mol) of **1b**.¹ This discrepancy could arise from any of the following effects: (1) the influence of the phenyl groups on the automerization rate; (2) an overestimation of the barrier at the MP2/3-21G//3-21G level, possibly due to limitations of the 3-21G basis set, the MP2 level of perturbation theory, or the closed-shell HF procedure;¹⁴ or (3) a contribution to the rate from quantum

(8) Butenhoff, T. J.; Moore, C. B. *J. Am. Chem. Soc.* **1988**, *110*, 8336.

(9) Merz, K. M., Jr.; Reynolds, C. H. *J. Chem. Soc., Chem. Commun.* **1988**, 90.

(10) Smedarchina, Z.; Siebrand, W.; Wildman, T. A. *Chem. Phys. Lett.* **1988**, *143*, 395.

(11) Rumpel, H.; Limbach, H.-H.; Zachmann, G. *J. Phys. Chem.* **1989**, *93*, 1812.

(12) Rumpel, H.; Limbach, H.-H. *J. Am. Chem. Soc.*, in press.

(13) (a) Dewar, M. J. S.; Thiel, W. *J. Am. Chem. Soc.* **1977**, *99*, 4899, 4907. (b) McKee, M. L.; Shevlin, P. B.; Rzepa, H. S. *J. Am. Chem. Soc.* **1986**, *108*, 5793.

(14) Rumpel and Limbach¹² have suggested the intermediacy of a singlet biradical, rather than a zwitterion, in this reaction, since they observe no kinetic solvent effects in solvents whose dielectric constants range from 2 to 25.

mechanical tunneling. Dewar and Merz² and Rumpel and Limbach¹² have suggested that tunneling contributions to the autoisomerization rate may occur via vibrationally assisted tunneling, i.e., direct conversion of a vibrationally excited state of **1** to the intermediate **2**.

Further work is in progress to study this reaction mechanism at higher levels of theory. While we do not believe that larger basis sets or more complete allowance for electron correlation will change the potential surface qualitatively, i.e., two-step versus concerted mechanism, they may serve to bring the theoretical and experimental activation barriers into better agreement.

Acknowledgment. We thank H.-H. Limbach for kindly providing us with preprints of ref 11 and 12. This research was conducted using the Merck IBM 3090/200 and the Rohm and Haas Alliant FX/80 computing facilities.

Supplementary Material Available: A table containing AM1 and 3-21G optimized geometries of **1a-4a** (2 pages). Ordering information is given on any current masthead page.

Photochemical C-H Bond Activation of Coordinated Propene in $(\eta^5\text{-C}_5\text{Me}_5)\text{Re}(\text{CO})_2(\eta^2\text{-C}_3\text{H}_6)$. X-ray Structure Determination of Exo and Endo Isomers of the Resulting η^3 -Allyl(hydrido) Complex $(\eta^5\text{-C}_5\text{Me}_5)\text{Re}(\text{H})(\text{CO})(\eta^3\text{-C}_3\text{H}_5)$

Raymond J. Batchelor, Frederick W. B. Einstein, Richard H. Jones, Jun-Ming Zhuang, and Derek Sutton*

Department of Chemistry, Simon Fraser University
Burnaby, British Columbia, Canada V5A 1S6
Received December 8, 1988

One mechanism that has been implicated in the transition-metal-catalyzed isomerization of alkenes is the reversible formation of an η^3 -allyl (hydrido) intermediate (Scheme I) by oxidative addition of an allylic C-H bond to the metal.¹⁻³ While a small number of well-characterized η^3 -allyl (hydrido) complexes have now been synthesized,²⁻¹¹ in no case has the crucial step of allylic C-H activation been observed starting from the well-defined alkene complex. To our knowledge, only one previous study mentions the photochemical formation of an η^3 -allyl (hydrido) complex.^{6,12} Here we report that photolysis of the propene

(1) Crabtree, R. H. *The Organometallic Chemistry of the Transition Metals*; Wiley-Interscience: New York, 1988; pp 188-190. Davies, S. G. *Organotransition Metal Chemistry: Applications to Organic Synthesis*; Pergamon Press: Oxford, 1982; Chapter 7. Collman, J. P.; Hegedus, L. S.; Norton, J. R.; Finke, R. G. *Principles and Applications of Organotransition Metal Chemistry*; University Science Books: Mill Valley, CA, 1987; p 175. Parshall, G. W. *Homogeneous Catalysis*; Wiley: New York, 1980; Chapter 3.

(2) (a) Tulip, T. H.; Ibers, J. A. *J. Am. Chem. Soc.* **1979**, *101*, 4201. (b) Tulip, T. H.; Ibers, J. A. *J. Am. Chem. Soc.* **1978**, *100*, 3252.

(3) (a) Sherman, E. O.; Olson, M. *J. Organomet. Chem.* **1979**, *172*, C13-C19. (b) Sherman, E. O.; Schreiner, P. R. *J. Chem. Soc., Chem. Commun.* **1978**, 223.

(4) (a) McGhee, W. S.; Bergman, R. G. *J. Am. Chem. Soc.* **1985**, *107*, 3388. (b) McGhee, W. S.; Bergman, R. G. *J. Am. Chem. Soc.* **1988**, *110*, 4246.

(5) Baudry, C.; Boydell, P.; Ephritikhine, M.; Felkin, H.; Guilhem, J.; Pascard, C.; Dau, E. T. H. *J. Chem. Soc., Chem. Commun.* **1985**, 670.

(6) Baudry, C.; Cormier, J. M.; Ephritikhine, M.; Felkin, H. *J. Organomet. Chem.* **1984**, *227*, 99.

(7) Thorn, D. L. *Organometallics* **1982**, *1*, 879.

(8) Chaudret, B. N.; Cole-Hamilton, D. J.; Wilkinson, G. *J. Am. Chem. Soc., Dalton Trans.* **1978**, 1739.

(9) Byrne, J. W.; Blaser, H. U.; Osborn, J. A. *J. Am. Chem. Soc.* **1975**, *97*, 3871.

(10) Siedle, A. R.; Newmark, R. A.; Brown-Wensley, K. A.; Skarjune, R. P.; Haddad, L. C. *Organometallics* **1988**, *7*, 2078.

(11) For examples of η^3 -allyl(hydrido) compounds stable only at low temperature or only observed spectroscopically in solution, see: (a) Howarth, O. W.; McAteer, C. H.; Moore, P.; Morris, G. E. *J. Chem. Soc., Chem. Commun.* **1981**, 506. (b) Bonnemant, H. *Angew. Chem., Int. Ed. Engl.* **1970**, *9*, 736. (c) Nixon, J. F.; Wilkins, B. *J. Organomet. Chem.* **1974**, *80*, 129. (d) Carturan, G.; Scriveranti, A.; Morandini, M. *Angew. Chem., Int. Ed. Engl.* **1981**, *20*, 112. Bertani, R.; Carturan, G.; Scriveranti, A. *Angew. Chem., Int. Ed. Engl.* **1983**, *22*, 246.

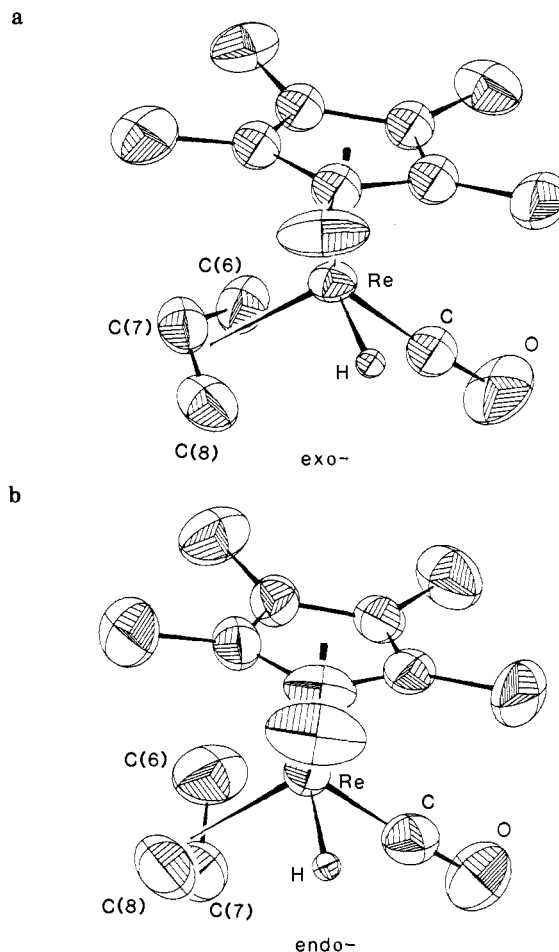
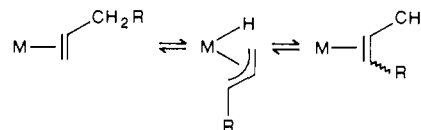
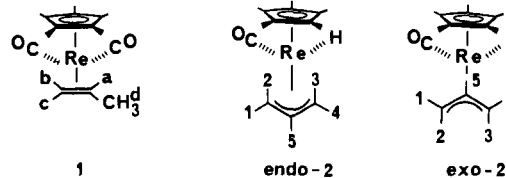


Figure 1. Perspective view of a molecule of *exo*- $(\eta^5\text{-C}_5\text{Me}_5)\text{Re}(\text{CO})(\text{H})(\eta^3\text{-C}_3\text{H}_5)$ (*exo-2*) (a) and of *endo*- $(\eta^5\text{-C}_5\text{Me}_5)\text{Re}(\text{CO})(\text{H})(\eta^3\text{-C}_3\text{H}_5)$ (*endo-2*) (b).

Scheme I



complex $\text{Cp}^*\text{Re}(\text{CO})_2(\text{C}_3\text{H}_6)$ (**1**) ($\text{Cp}^* = \eta^5\text{-C}_5\text{Me}_5$) results in the formation of the η^3 -allyl (hydrido) complex $\text{Cp}^*\text{Re}(\text{CO})(\text{H})(\eta^3\text{-C}_3\text{H}_5)$ (**2**). Furthermore, we have been successful in isolating the *exo* and *endo* isomers of **2**, differing in the orientation of the η^3 -allyl group, and the structures of both have been determined by X-ray crystallography.



Irradiation of $\text{Cp}^*\text{Re}(\text{CO})_3$ in hexane in a quartz tube at 0 °C for 1 h with a propene purge resulted in an IR spectrum having strong absorptions at 1890 and 1961 cm^{-1} for the propene complex **1** and weaker ones at 1904 and 1912 cm^{-1} for *exo-2* and *endo-2*

(12) We are informed of a related unpublished synthesis of $(\eta^5\text{-C}_5\text{H}_5)\text{Re}(\text{H})(\text{CO})(\eta^3\text{-C}_3\text{H}_5)$ done in Professor W. A. G. Graham's laboratory at the University of Alberta: Graham, W. A. G., private communication.